



# Schisandrin B regulates macrophage polarization and alleviates liver fibrosis via activation of PPAR $\gamma$

Qingshan Chen<sup>1</sup>, Leilei Bao<sup>1</sup>, Lei Lv<sup>1</sup>, Fangyuan Xie<sup>1</sup>, Xuwei Zhou<sup>2</sup>, Hai Zhang<sup>3</sup>, Guoqing Zhang<sup>1</sup>

<sup>1</sup>Department of Pharmacy, Third Affiliated Hospital of Naval Military Medical University, Shanghai, China; <sup>2</sup>Department of Basic Medicine, Fudan University School of Medicine, Shanghai, China; <sup>3</sup>Department of Pharmacy, Shanghai First Maternity and Infant Hospital, Tong Ji University School of Medicine, Shanghai, China

**Contributions:** (I) Conception and design: Q Chen, H Zhang; (II) Administrative support: G Zhang, L Bao; (III) Provision of study materials or patients: Q Chen, H Zhang; (IV) Collection and assembly of data: L Lv, F Xie; (V) Data analysis and interpretation: Q Chen, X Zhou; (VI) Manuscript writing: All authors; (VII) Final approval of manuscript: All authors.

**Correspondence to:** Guoqing Zhang. Department of Pharmacy, Third Affiliated Hospital of Naval Military Medical University, Shanghai, China. Email: gqzhang@smmu.edu.cn; Hai Zhang. Department of Pharmacy, Shanghai First Maternity and Infant Hospital, Tong Ji University School of Medicine, Shanghai, China. zhxdks2005@126.com.

**Background:** Schisandrin B (Sch B), the main ingredient of *Schisandra chinensis*, displays many bioactivities. This study aimed to identify the drug target of Sch B against liver fibrosis and describe the related molecular mechanisms.

**Methods:** The effects of Sch B on liver fibrosis and macrophage polarization was investigated *in vivo* and *in vitro*. Furthermore, we analyzed the regulatory effect of Sch B on peroxisome proliferator-activated receptor gamma (PPAR $\gamma$ ).

**Results:** Our data showed that Sch B dramatically alleviated liver inflammation and fibrosis and inhibited macrophage activation via PPAR $\gamma$ . Sch B binds with PPAR $\gamma$  by molecular docking. Immunofluorescence double staining showed that PPAR $\gamma$  was mainly expressed in macrophages rather than hepatic stellate cells (HSCs) in liver fibrosis. Importantly, Sch B strongly inhibited macrophage polarization in fibrotic livers compared with the model group. Further, the results revealed that Sch B efficiently inhibited macrophage polarization and also decreased the levels of inflammatory cytokines *in vitro*. Knockdown of PPAR $\gamma$  by small interfering RNA (siRNA) inhibited the effect of Sch B on macrophage polarization. Mechanistically, Sch B regulated macrophage polarization through inhibition of the nuclear factor (NF)- $\kappa$ B signaling pathway via PPAR $\gamma$  both *in vivo* and *in vitro*.

**Conclusions:** These results suggested that Sch B alleviated carbon tetrachloride (CCl<sub>4</sub>)-induced liver inflammation and fibrosis by inhibiting macrophage polarization via targeting PPAR $\gamma$ .

**Keywords:** Schisandrin B; liver fibrosis; macrophage polarization; peroxisome proliferator-activated receptor gamma (PPAR $\gamma$ )

Submitted Aug 06, 2021. Accepted for publication Sep 27, 2021.

doi: 10.21037/atm-21-4602

View this article at: <https://dx.doi.org/10.21037/atm-21-4602>

## Introduction

Schisandrin B (Sch B), the main bioactive ingredient of *Schisandra chinensis*, has been used in Asia for centuries to treat chronic liver disease resulting from hepatitis virus infection (1-4). Liver fibrosis is characterized by excessive deposition of extracellular matrix (ECM) at the injury site, which can lead to liver failure. However, few treatment options are currently available (5-8) and therefore, the development

of new therapeutic drugs for liver fibrosis, along with an understanding of the molecular mechanisms involved, is vitally important. In our previous studies, we found that Sch B mitigated carbon tetrachloride (CCl<sub>4</sub>)-induced liver fibrosis in rats by blocking the transforming growth factor beta (TGF- $\beta$ )/Smad signaling pathway (9). However, the potential molecular mechanisms of Sch B against liver fibrosis remain unclear, and the drug target of Sch B is unknown.

Hepatic stellate cells (HSCs) are the most important cell type involved in the development and progression of liver fibrosis (6,10). HSCs are activated by inflammatory cytokines and secrete large amounts of collagen protein, leading to excessive deposition of ECM (8). HSCs have become an important therapeutic target for liver fibrosis. Hepatic macrophages have also been found to perform a function in the progression and regression of liver fibrosis (11). Macrophages are highly heterogeneous immune cells which have a proinflammatory M1 phenotype and an anti-inflammatory M2 phenotype (12,13). M1 macrophages promote the pathological process of liver fibrosis by producing proinflammatory cytokines, while M2 macrophages inhibit the activation of M1 macrophages to exert an anti-liver fibrosis effect. Several studies have demonstrated that Sch B inhibits inflammation (14-18), and previous research findings have confirmed that the anti-inflammatory effects of Sch B are closely related to inhibition of macrophage activation and activation of the antioxidant system (14,19). However, in the process of liver fibrosis, it is not clear whether the anti-inflammatory effect of Sch B is related to the activation of macrophages.

Previously, we used RNA sequencing to show that Sch B protects against liver fibrosis through multiple mechanisms, including antioxidant and anti-inflammatory activities, inhibition of endoplasmic reticulum stress, and regulation of immune response (20). Further, we found that the peroxisome proliferator-activated receptor gamma (PPAR $\gamma$ ) signaling pathway was the main target of Sch B. Several studies have reported that PPAR $\gamma$  alleviates inflammatory response, liver fibrosis, and nonalcoholic fatty liver disease (NAFLD) through the inhibition of HSC activation and Kupffer cell polarization (21-24). However, the role of Sch B on the PPAR $\gamma$  pathway and macrophage polarization *in vivo* and *in vitro* remains unclear. In this study, we investigated the effect of Sch B on the PPAR $\gamma$  pathway and macrophage polarization and clarified its underlying molecular mechanisms. In particular, we focused on the cellular localization and biological function of PPAR $\gamma$  in liver fibrosis. We present the following article in accordance with the ARRIVE reporting checklist (available at <https://dx.doi.org/10.21037/atm-21-4602>).

## Methods

### Reagents

Sch B was purchased from Selleck Chemicals (Houston,

TX, USA). Carbon tetrachloride (CCl $_4$ ) was purchased from Chinasun Specialty Products Co., Ltd. (Changshu, Jiangsu, China). Lipopolysaccharide (LPS) was purchased from Sigma-Aldrich (St. Louis, MO, USA). Rabbit anti-PPAR $\gamma$ , anti-F4/80, anti-alpha smooth muscle actin ( $\alpha$ -SMA), anti-CD86, Lamin B1, and glyceraldehyde 3-phosphate dehydrogenase (GAPDH) antibodies were obtained from Affinity Biosciences (Changzhou, Jiangsu, China). Rabbit antibodies against nuclear factor (NF)- $\kappa$ B and phospho-I $\kappa$ B $\alpha$  were purchased from Cell Signaling Technology (Danvers, MA, USA). Secondary antibodies used in western blotting and immunohistochemical staining were purchased from Affinity Biosciences. Secondary antibodies used in immunofluorescence staining were purchased from Abcam (Cambridge, MA, USA).

### Cell culture and experimental design

Murine macrophage RAW264.7 cell line was purchased from the Cell Bank of the Chinese Academy of Sciences (Shanghai, China). RAW264.7 cells were cultured in Dulbecco's modified Eagle's medium (DMEM) solution, supplemented with 10% fetal bovine serum (FBS), 100 U/mL penicillin, and 100  $\mu$ g/mL streptomycin at 37 °C in a 5% CO $_2$  atmosphere.

We used LPS to induce macrophage M1 differentiation to assess the effects of Sch B on macrophage activation. Cells were cultured in 24-well plates overnight. After 24 hours, cells were serum-starved and treated with LPS and Sch B (10, 30, and 50  $\mu$ M) for an additional 24-hour period. Subsequently, the cell supernatant was collected and the levels of inflammatory cytokines were detected using an enzyme-linked immunosorbent assay (ELISA) according to the instruction manual.

Further, we induced PPAR $\gamma$  expression knockdown using small interfering RNA (siRNA) transfection. RNAiMAX and siRNA transfection reagent INTERFERin were premixed in antibiotic-free medium according to the instruction manual. Once RAW264.7 cells reached about 50% density, we started transfecting PPAR $\gamma$  siRNA (GenePharma, Shanghai, China). After 24 hours of transfection, the cell medium was replaced by DMEM with 10% FBS.

### Docking experiment

The crystal structure of PPAR $\gamma$  was obtained from the Protein Data Bank (PDB ID: 3R8A) (25). Water molecules were removed from the structure. The docking site selection

was based on the 5 Å amino acid residues surrounding the original ligand. Molecular docking was performed using the CDOCKER module of Discovery Studio 2016 (Accelrys, San Diego, USA). The number of top hits was set as 30 and the pose cluster radius was set to 0.1. The best pose was selected according to CDOCKER energy value. The binding results were visualized in PyMol.

### *Animal experiments*

Male Sprague-Dawley rats weighing 150–200 g were purchased from the Shanghai Laboratory Animal Center (Shanghai, China). The rats were housed under appropriate temperature ( $25 \pm 2$  °C), humidity (50–60%), and light conditions (12-hour light/dark cycle). Experiments were performed under a project license (No. 20194Y0357) granted by ethics committee of the Naval Military Medical University, in compliance with the Naval Military Medical University guidelines for the care and use of animals.

The rats were randomly assigned to the control group, model group, and Sch B group (25 or 50 mg/kg). Each group contained 8 rats. Liver fibrosis rats received intragastrical administration of  $\text{CCl}_4$  (50%  $\text{CCl}_4$  dissolved in olive oil; 2 mL/kg) twice a week for 8 weeks. Rats in the Sch B group were administered  $\text{CCl}_4$  for 4 weeks and then treated with Sch B at a dose of either 25 or 50 mg/kg daily, respectively. In the control group, rats received an equal volume of olive oil. At the end of the experiment, rats were sacrificed with pentobarbital sodium, and liver tissue was collected for further analysis.

### *Histological analysis*

We used hematoxylin/eosin (H&E), Sirius Red, and Masson's trichrome staining to conduct histological examinations, using methods described previously (9,20). The area density of collagen deposition was quantified by Image-Pro Plus 6.0 software. Pathological sections were photographed and recorded by microscopy (Olympus, Tokyo, Japan).

### *Immunofluorescence staining*

A detailed description of the immunofluorescence staining method was included in our previous study (26). Briefly, liver tissue sections were deparaffinized and blocked in phosphate-buffered saline (PBS) with 3% bovine serum albumin (BSA). The sections were labeled with primary antibodies F4/80 (1:200 dilution) and  $\alpha$ -SMA (1:200

dilution) overnight at 4 °C and subsequently incubated with antibody PPAR $\gamma$  (1:100 dilution) for double staining. Next, the fluorescent secondary conjugated Alexa Fluor-488 and Alexa Fluor-555 were incubated at room temperature for 2 hours. After washing, the cell nuclei were counterstained with 4',6-diamidino-2-phenylindole (DAPI). Finally, the stained sections were analyzed via fluorescence microscopy (BX51, Olympus, Japan).

### *Immunohistochemistry staining analysis*

Paraffin-embedded liver sections were dewaxed, hydrated, and subjected to antigen retrieval according to standard protocols as previously described (26,27). Nonspecific protein was blocked by 5% BSA. Subsequently, the sections were incubated with primary antibodies CD86 (1:200 dilution) overnight at 4 °C. The sections were washed with PBS and incubated with horseradish peroxidase (HRP)-conjugated goat anti-rabbit secondary antibodies. Finally, the liver tissue sections were stained with 3,3'-diaminobenzidine tetrahydrochloride (DAB) and visualized by light microscope.

### *Western blot analysis*

Western blot analysis was performed as previously described (9). The nuclear and cytoplasmic protein from RAW264.7 cells were extracted using a Protein Extraction Kit (Beyotime Biotechnology, Jiangsu, China). Protein concentration was quantified by the Bradford method. Equal amounts of proteins were then separated by sodium dodecyl sulphate-polyacrylamide gel electrophoresis (SDS-PAGE) and transferred onto nitrocellulose membranes. Immunoblotting was conducted using the following antibodies: rabbit anti-PPAR $\gamma$  (1:200 dilution), NF- $\kappa$ B p65 (1:200 dilution), phospho-I $\kappa$ B $\alpha$  (1:200 dilution), histone H3 (1:500 dilution), and  $\beta$ -actin (1:500 dilution) at 4 °C overnight. The membranes were washed the next day and then incubated with secondary antibody at room temperature. The western blot bands were visualized using an enhanced chemiluminescence system (Fusion FX7 Spectra, Vilber Lourmat, Eberhardzell, Germany) and then analyzed using Quantity One software (Bio-Rad Laboratories, CA, USA) according to standard methods.

### *Statistical analysis*

The data are presented as the mean  $\pm$  SD. Comparisons

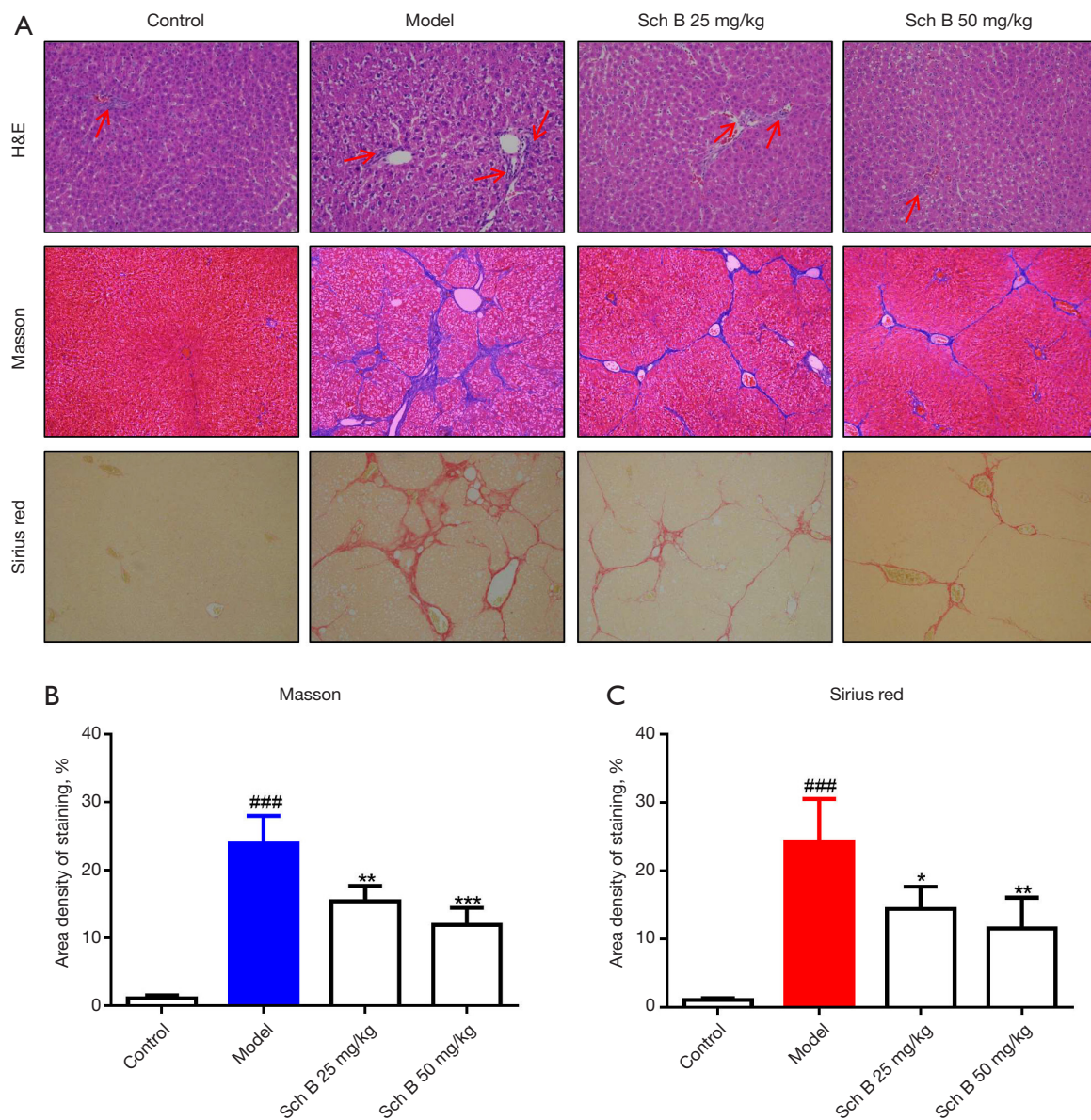


**Figure 1** Sch B prevents CCl<sub>4</sub>-induced liver fibrosis. (A) H&E staining, Masson's trichrome staining, and Sirius red staining of liver sections, the red arrows represent the pathological morphology of liver tissue, magnification:  $\times 100$ . (B) The area of Masson's trichrome staining in liver (%). (C) The area of Sirius red staining in liver (%). Data are mean  $\pm$  SD (n=8). ###, P<0.001 versus the control group; \*, P<0.05, \*\*, P<0.01, \*\*\*, P<0.001 versus the model group.

were performed using one-way ANOVA in GraphPad Prism 5. A value of P<0.05 was considered statistically significant.

## Results

### Sch B prevents CCl<sub>4</sub>-induced liver fibrosis

We used histopathological methods to evaluate the

protective effect of Sch B on CCl<sub>4</sub>-induced liver fibrosis in rats. After 2 months of treatment with CCl<sub>4</sub>, liver fibrosis with symptoms occurred, including liver necrosis and collagen deposition. As shown in *Figure 1A*, CCl<sub>4</sub> treatment resulted in severe liver damage, as indicated by the large area of hepatocyte ballooning degeneration and partial inflammatory cell infiltration in the model group.

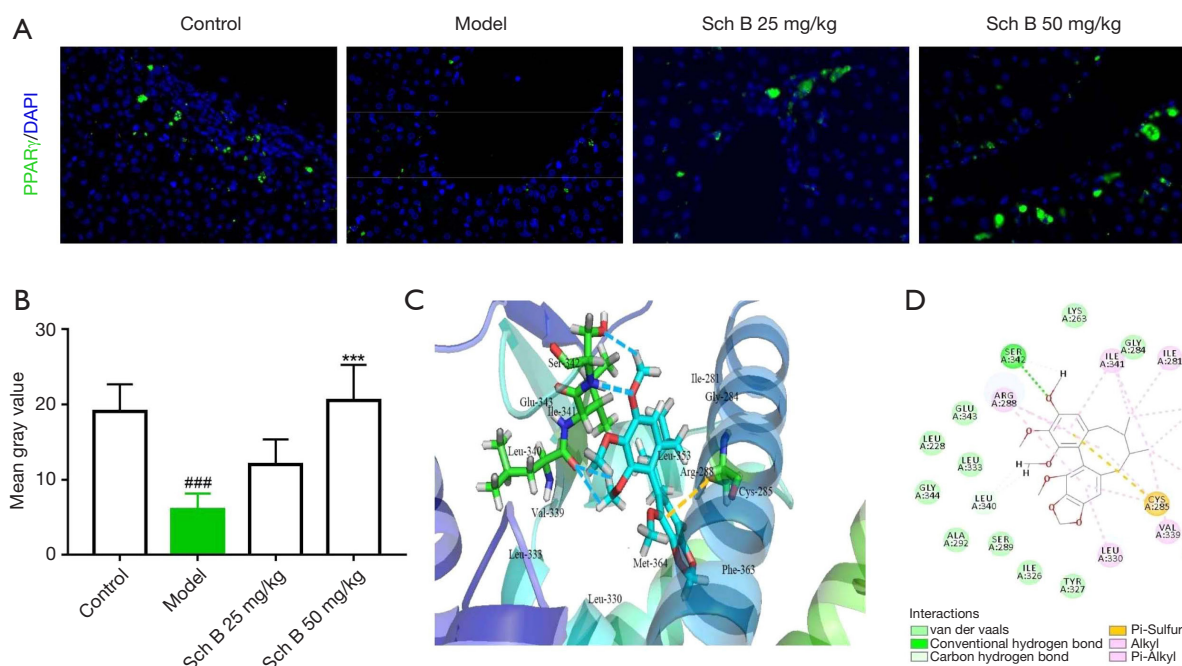


**Figure 2** PPAR $\gamma$  is the target of Sch B against liver fibrosis. (A) Immunofluorescence staining of PPAR $\gamma$  and DAPI in liver tissue, magnification:  $\times 200$ . (B) Immunofluorescence intensity of PPAR $\gamma$  in liver tissue (%). (C) Three-dimensional diagram of Sch B binding with PPAR $\gamma$ . (D) Two-dimensional diagram of Sch B in the active site of PPAR $\gamma$ . <sup>###</sup>,  $P < 0.001$  versus the control group; <sup>\*\*\*</sup>,  $P < 0.001$  versus the model group. PPAR $\gamma$ , peroxisome proliferator-activated receptor gamma; Sch B, Schisandrin B; DAPI, 4',6-diamidino-2-phenylindole.

The results of H&E staining confirmed that the liver injury was significantly attenuated by treatment with Sch B (25 and 50 mg/kg). Further, Masson's trichrome and Sirius red staining confirmed that CCl<sub>4</sub> treatment caused a significant deposition of ECM and collagen in the liver fibrosis model group (Figure 1A). As expected, Sch B treatment significantly decreased collagen deposition, with about 25% decrease in the 25 mg/kg group and about 55% decrease in the 50 mg/kg group (Figure 1B,1C). Overall, these results suggested that Sch B protected against CCl<sub>4</sub>-induced liver injury and liver fibrosis.

### PPAR $\gamma$ is the target of Sch B against liver fibrosis

As previous transcriptomic studies have shown that Sch B regulated the PPAR $\gamma$  signaling pathway, we theorized that PPAR $\gamma$  may be the target of Sch B against liver fibrosis. In this study, we first used immunofluorescence staining to detect the expression of PPAR $\gamma$  to examine whether PPAR $\gamma$  was involved in Sch B-mediated anti-liver fibrosis effects. As shown in Figure 2A,2B, compared with the control group, the expression of PPAR $\gamma$  was significantly decreased in the model group ( $P < 0.001$ ). However, Sch B treatment activated

CCl<sub>4</sub>-induced inhibition of the PPAR $\gamma$  signaling pathway and reversed the decreased levels of PPAR $\gamma$ . Further, molecular docking was performed to explore the interaction mechanisms of Sch B on PPAR $\gamma$ . As shown in Figure 2C,2D, Sch B was able to bind with PPAR $\gamma$  in the binding pocket region between H3 and the  $\beta$ -sheet, which has a hydrophobic entrance and interior. The main sites of Sch B interaction with PPAR $\gamma$  were ARG288, SER342, ILE341, ILE281, MET348, LEU353, CYS285, VAL339, and LEU330.

### Sch B inhibits macrophage activation and inflammation via PPAR $\gamma$

Previous studies have indicated that PPAR $\gamma$  in HSCs or macrophages played an important role in the progression of liver fibrosis. To determine which cell (HSC or macrophage) mainly expressed PPAR $\gamma$ , immunofluorescence double staining of PPAR $\gamma$  and F4/80 (macrophage marker) or  $\alpha$ -SMA (HSC marker) were performed on liver sections. As shown in Figure 3A, the results clearly showed that there was a greater coexpression of PPAR $\gamma$  and macrophage marker F4/80 in liver fibrosis tissue relative to the control group. We did not observe coexpression of PPAR $\gamma$  and HSC

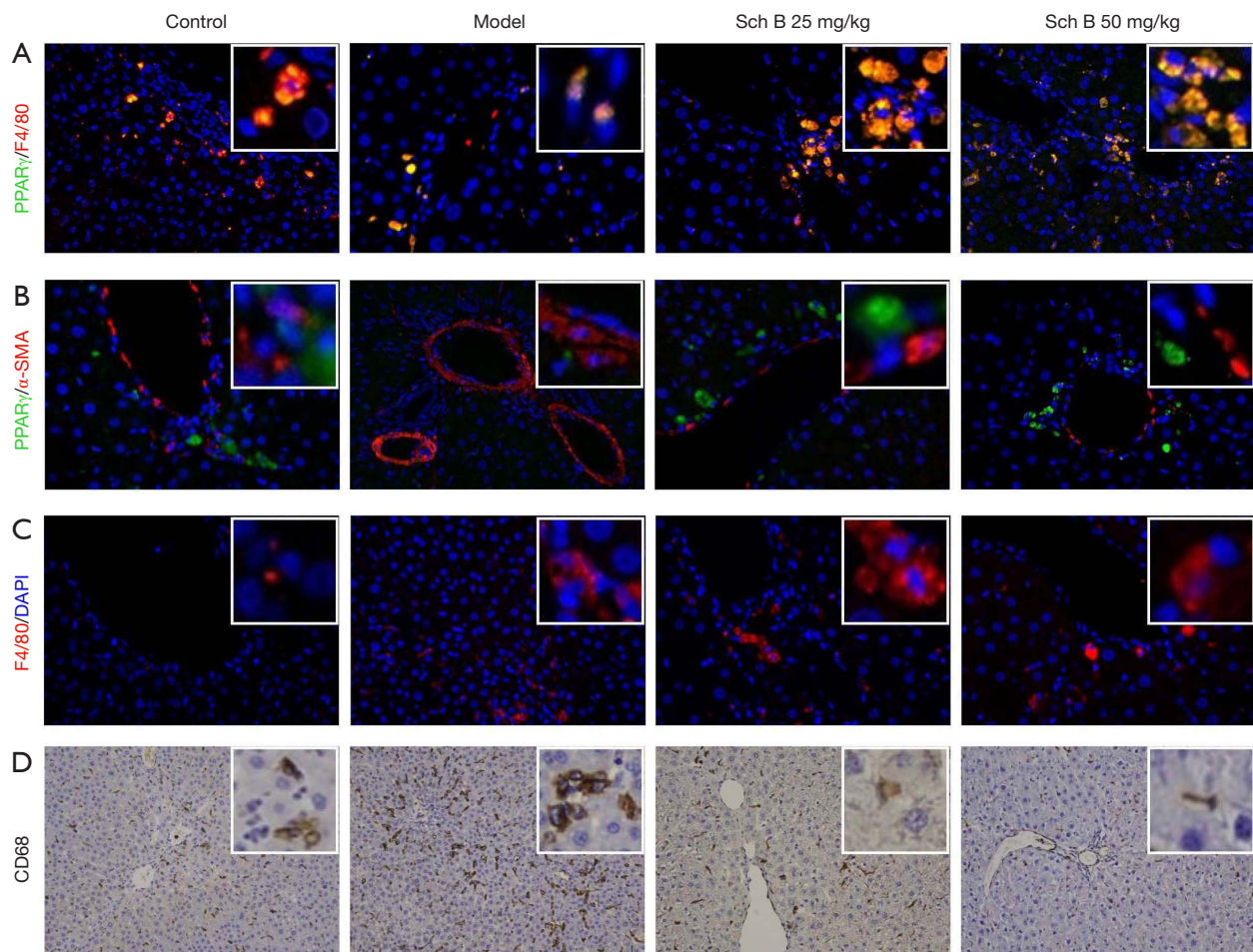


**Figure 3** Sch B inhibits macrophage activation via PPAR $\gamma$ . (A) Immunofluorescence staining of PPAR $\gamma$  and F4/80 in liver tissue; the nuclei were stained with DAPI (blue); magnification:  $\times 200$ . (B) Immunofluorescence staining of PPAR $\gamma$  and  $\alpha$ -SMA in liver tissue; the nuclei were stained with DAPI (blue); magnification:  $\times 200$ . (C) Immunofluorescence staining of F4/80 in liver tissue; the nuclei were stained with DAPI (blue); magnification:  $\times 200$ . (D) Immunohistochemistry staining of CD68 in liver tissue, magnification:  $\times 200$ . Sch B, Schisandrin B; PPAR $\gamma$ , peroxisome proliferator-activated receptor gamma; DAPI, 4',6-diamidino-2-phenylindole.

marker  $\alpha$ -SMA in liver fibrosis tissue sections (Figure 3B). As macrophages are closely related to inflammation, we subsequently evaluated the effects of Sch B on inflammation. The expression of F4/80 and CD68 were increased in the liver tissue of liver fibrosis mice compared with the control group (Figure 3C,3D). These data strongly indicated that Sch B inhibited macrophage activation and inflammation via PPAR $\gamma$ .

#### ***PPAR $\gamma$ is necessary for Sch B inhibition of macrophage activation in vitro***

We further verified the inhibitory effect of Sch B on

inflammation by using LPS stimulating RAW264.7 cells *in vitro*. Consistent with the effect of Sch B *in vivo*, the results of ELISA analysis showed that Sch B strongly inhibited LPS-induced secretion of inflammatory cytokines tumor necrosis factor (TNF)- $\alpha$ , interleukin (IL)-6, and IL-1 $\beta$  levels (Figure 4A-4C). Importantly, to confirm whether PPAR $\gamma$  was the biological target of Sch B inhibition of macrophage activation, we used siRNA to silence PPAR $\gamma$  expression via the transfection of RAW264.7 cells. As shown in Figure 4D-4F, Sch B decreased LPS-induced secretion of TNF- $\alpha$ , IL-6, and IL-1 $\beta$  in the RAW264.7 cells, whereas the reduction was reversed by PPAR $\gamma$  siRNA. These results indicated that Sch B inhibited macrophage activation via

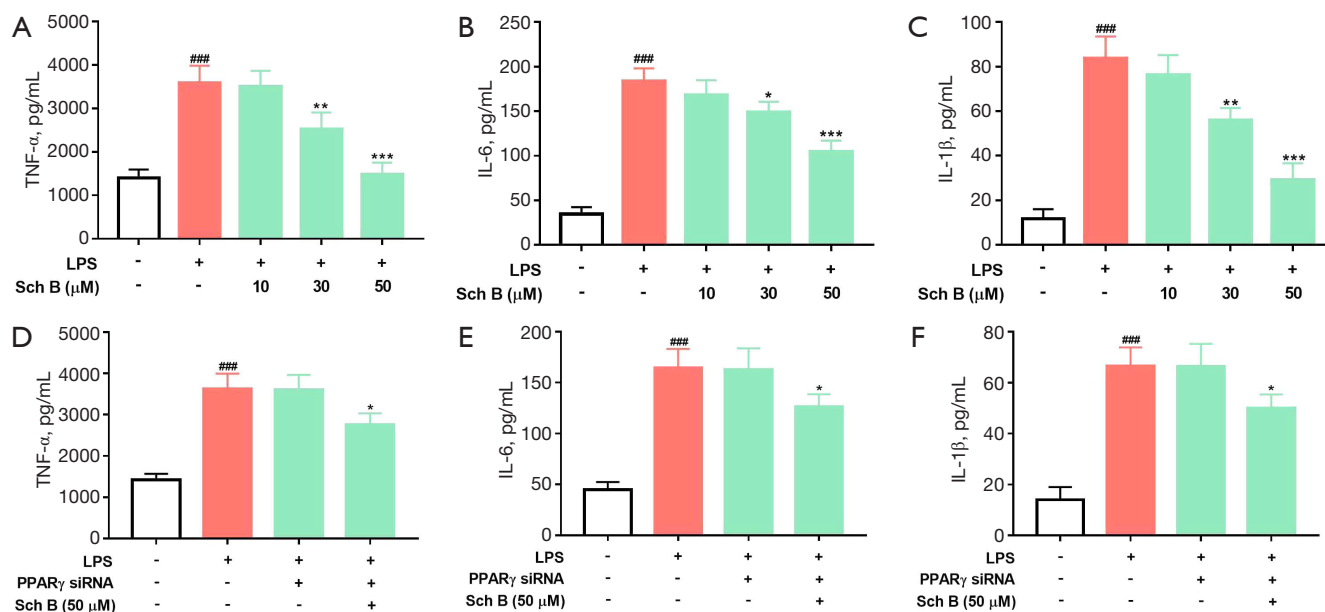


**Figure 4** PPAR $\gamma$  is necessary for Sch B inhibition of macrophage activation *in vitro*. (A-C) The TNF- $\alpha$ , IL-6, and IL-1 $\beta$  content of Sch B inhibits LPS-induced RAW264.7 cells, respectively. (D-F) The TNF- $\alpha$ , IL-6, and IL-1 $\beta$  content of treatment with PPAR $\gamma$  siRNA in RAW264.7 cells, respectively. Data are expressed as the mean  $\pm$  SD (n=3). ###, P<0.001 versus the control group; \*, P<0.05, \*\*, P<0.01, \*\*\*, P<0.001 versus the model group. PPAR $\gamma$ , peroxisome proliferator-activated receptor gamma; Sch B, Schisandrin B; TNF- $\alpha$ , tumor necrosis factor- $\alpha$ ; IL, interleukin; LPS, lipopolysaccharide.

PPAR $\gamma$ , suggesting that PPAR $\gamma$  is the biological target of Sch B inhibition of macrophage activation.

#### Sch B inhibits NF- $\kappa$ B signaling via the PPAR $\gamma$ /p65 complex

It is widely accepted that the NF- $\kappa$ B signaling pathway plays a critical role in macrophage activation and inflammation during liver fibrosis. Therefore, we investigated the NF- $\kappa$ B signaling pathway to determine whether it was involved in the Sch B-mediated inhibition of macrophage activation and anti-liver fibrosis effects. We found that in the LPS-induced macrophage activation model, the expression of p65 and phosphorylation of I $\kappa$ B $\alpha$  (p-I $\kappa$ B $\alpha$ ) were significantly increased in the nucleus and cytoplasm, respectively. However, Sch B treatment suppressed LPS-induced activation of the NF- $\kappa$ B signaling pathway and decreased the expression of p65 and p-I $\kappa$ B $\alpha$  in a dose-dependent manner (Figure 5A,5B). Meanwhile, the expression of PPAR $\gamma$  remained unchanged (Figure 5A,5B). Further, immunofluorescence staining clearly showed that Sch B treatment decreased the expression of phosphorylation of p65 (p-p65) and inhibited the NF- $\kappa$ B signaling pathway

(Figure 5C). These results suggested that Sch B protected against liver fibrosis by inhibiting the NF- $\kappa$ B signaling pathway.

#### Discussion

Our previous research reported that Sch B inhibited the TGF- $\beta$ /Smad signaling pathway and HSC activation to attenuate liver fibrosis (9). However, the molecular mechanisms underlying the effect of Sch B against liver fibrosis remain largely unclear. In order to clarify the drug target of Sch B, we used transcriptome RNA sequencing and found that PPAR $\gamma$  is an important signaling pathway. Importantly, molecular docking analysis found that Sch B binds to PPAR $\gamma$ . In this study, our results suggested that Sch B protected against CCl $_4$ -induced liver fibrosis in mice by inhibiting the NF- $\kappa$ B signaling pathway and macrophage activation through activation of PPAR $\gamma$ . The findings of this study were consistent with previous studies and further demonstrated that PPAR $\gamma$  and macrophages are the drug target and target cells of Sch B, respectively.

In our study, H&E, Masson's trichrome, and Sirius red staining clearly reflected that Sch B could attenuate chronic





was significantly attenuated, suggesting that the anti-liver fibrosis effect of Sch B was related to the suppression of the NF- $\kappa$ B signaling pathway.

In conclusion, our study demonstrated that PPAR $\gamma$  was the target of Sch B, a natural compound which has been shown to protect against liver fibrosis. Further, we found that PPAR $\gamma$  was mainly expressed in macrophages in liver fibrosis and was the key to macrophage activation. Finally, we found that Sch B suppressed the NF- $\kappa$ B/I $\kappa$ B $\alpha$  pathway to inhibit macrophage activation by PPAR $\gamma$ . These results suggested that Sch B has therapeutic potential against liver fibrosis through the activation of PPAR $\gamma$ .

### Acknowledgments

*Funding:* This work was financially supported by the Clinical Research Project of Shanghai Municipal Health Commission (No. 20194Y0357), the Fund of Naval Military Medical University (2018QN17), and the National Natural Science Foundation of China (No. 81773797; No. 81903843). We also thank for the support of the talent project of Wu Mengchao.

### Footnote

*Reporting Checklist:* The authors have completed the ARRIVE reporting checklist. Available at <https://dx.doi.org/10.21037/atm-21-4602>

*Data Sharing Statement:* Available at <https://dx.doi.org/10.21037/atm-21-4602>

*Conflicts of Interest:* All authors have completed the ICMJE uniform disclosure form (available at <https://dx.doi.org/10.21037/atm-21-4602>). The authors have no conflicts of interest to declare.

*Ethical Statement:* The authors are accountable for all aspects of the work in ensuring that questions related to the accuracy or integrity of any part of the work are appropriately investigated and resolved. Experiments were performed under a project license (No. 20194Y0357) granted by ethics committee of the Naval Military Medical University, in compliance with the Naval Military Medical University guidelines for the care and use of animals.

*Open Access Statement:* This is an Open Access article distributed in accordance with the Creative Commons

Attribution-NonCommercial-NoDerivs 4.0 International License (CC BY-NC-ND 4.0), which permits the non-commercial replication and distribution of the article with the strict proviso that no changes or edits are made and the original work is properly cited (including links to both the formal publication through the relevant DOI and the license). See: <https://creativecommons.org/licenses/by-nc-nd/4.0/>.

### References

1. Nasser MI, Zhu S, Chen C, et al. A Comprehensive Review on Schisandrin B and Its Biological Properties. *Oxid Med Cell Longev* 2020;2020:2172740.
2. Hong M, Zhang Y, Li S, et al. A Network Pharmacology-Based Study on the Hepatoprotective Effect of Fructus Schisandrae. *Molecules* 2017;22:1617.
3. Panossian A, Wikman G. Pharmacology of Schisandra chinensis Bail.: an overview of Russian research and uses in medicine. *J Ethnopharmacol* 2008;118:183-212.
4. Fan X, Jiang Y, Wang Y, et al. Wuzhi tablet (Schisandra Sphenanthera extract) protects against acetaminophen-induced hepatotoxicity by inhibition of CYP-mediated bioactivation and regulation of NRF2-ARE and p53/p21 pathways. *Drug Metab Dispos* 2014;42:1982-90.
5. Cao Y, Ji C, Lu L. Mesenchymal stem cell therapy for liver fibrosis/cirrhosis. *Ann Transl Med* 2020;8:562.
6. Tsuchida T, Friedman SL. Mechanisms of hepatic stellate cell activation. *Nat Rev Gastroenterol Hepatol* 2017;14:397-411.
7. Pellicoro A, Ramachandran P, Iredale JP, et al. Liver fibrosis and repair: immune regulation of wound healing in a solid organ. *Nat Rev Immunol* 2014;14:181-94.
8. Roohani S, Tacke F. Non-invasive assessment for alpha-1 antitrypsin deficiency-associated liver disease: new insights on steatosis and fibrosis in Pi\*ZZ carriers. *Transl Gastroenterol Hepatol* 2019;4:82.
9. Chen Q, Zhang H, Cao Y, et al. Schisandrin B attenuates CCl4-induced liver fibrosis in rats by regulation of Nrf2-ARE and TGF- $\beta$ /Smad signaling pathways. *Drug Des Devel Ther* 2017;11:2179-91.
10. Higashi T, Friedman SL, Hoshida Y. Hepatic stellate cells as key target in liver fibrosis. *Adv Drug Deliv Rev* 2017;121:27-42.
11. Tacke F. Targeting hepatic macrophages to treat liver diseases. *J Hepatol* 2017;66:1300-12.
12. Li H, You H, Fan X, et al. Hepatic macrophages in liver fibrosis: pathogenesis and potential therapeutic targets. *BMJ Open Gastroenterol* 2016;3:e000079.

13. Ramachandran P, Pellicoro A, Vernon MA, et al. Differential Ly-6C expression identifies the recruited macrophage phenotype, which orchestrates the regression of murine liver fibrosis. *Proc Natl Acad Sci U S A* 2012;109:E3186-95.
14. Leong PK, Wong HS, Chen J, et al. Differential Action between Schisandrin A and Schisandrin B in Eliciting an Anti-Inflammatory Action: The Depletion of Reduced Glutathione and the Induction of an Antioxidant Response. *PLoS One* 2016;11:e0155879.
15. Lin Q, Qin X, Shi M, et al. Schisandrin B inhibits LPS-induced inflammatory response in human umbilical vein endothelial cells by activating Nrf2. *Int Immunopharmacol* 2017;49:142-7.
16. Ran J, Ma C, Xu K, et al. Schisandrin B ameliorated chondrocytes inflammation and osteoarthritis via suppression of NF- $\kappa$ B and MAPK signal pathways. *Drug Des Devel Ther* 2018;12:1195-204.
17. Ma Z, Xu G, Shen Y, et al. Schisandrin B-mediated TH17 cell differentiation attenuates bowel inflammation. *Pharmacol Res* 2021;166:105459.
18. Chen X, Xiao Z, Jiang Z, et al. Schisandrin B Attenuates Airway Inflammation and Airway Remodeling in Asthma by Inhibiting NLRP3 Inflammasome Activation and Reducing Pyroptosis. *Inflammation* 2021. [Epub ahead of print]. doi: 10.1007/s10753-021-01494-z.
19. Leong PK, Ko KM. Schisandrin B induces an Nrf2-mediated thioredoxin expression and suppresses the activation of inflammasome in vitro and in vivo. *Biofactors* 2015;41:314-23.
20. Zhang H, Chen Q, Dahan A, et al. Transcriptomic analyses reveal the molecular mechanisms of schisandrin B alleviates CCl4-induced liver fibrosis in rats by RNA-sequencing. *Chem Biol Interact* 2019;309:108675.
21. Wang Z, Xu JP, Zheng YC, et al. Peroxisome proliferator-activated receptor gamma inhibits hepatic fibrosis in rats. *Hepatobiliary Pancreat Dis Int* 2011;10:64-71.
22. Han X, Wu Y, Yang Q, et al. Peroxisome proliferator-activated receptors in the pathogenesis and therapies of liver fibrosis. *Pharmacol Ther* 2021;222:107791.
23. Zhang F, Lu Y, Zheng S. Peroxisome proliferator-activated receptor- $\gamma$  cross-regulation of signaling events implicated in liver fibrogenesis. *Cell Signal* 2012;24:596-605.
24. Wu L, Li J, Feng J, et al. Crosstalk between PPARs and gut microbiota in NAFLD. *Biomed Pharmacother* 2021;136:111255.
25. Casimiro-Garcia A, Filzen GF, Flynn D, et al. Discovery of a series of imidazo[4,5-b]pyridines with dual activity at angiotensin II type 1 receptor and peroxisome proliferator-activated receptor- $\gamma$ . *J Med Chem* 2011;54:4219-33.
26. Wei L, Chen Q, Guo A, et al. Asiatic acid attenuates CCl4-induced liver fibrosis in rats by regulating the PI3K/AKT/mTOR and Bcl-2/Bax signaling pathways. *Int Immunopharmacol* 2018;60:1-8.
27. Fan J, Chen Q, Wei L, et al. Asiatic acid ameliorates CCl4-induced liver fibrosis in rats: involvement of Nrf2/ARE, NF- $\kappa$ B/I $\kappa$ B $\alpha$ , and JAK1/STAT3 signaling pathways. *Drug Des Devel Ther* 2018;12:3595-605.
28. Montaigne D, Butruille L, Staels B. PPAR control of metabolism and cardiovascular functions. *Nat Rev Cardiol* 2021. [Epub ahead of print]. doi: 10.1038/s41569-021-00569-6.
29. Mirza AZ, Althagafi II, Shamshad H. Role of PPAR receptor in different diseases and their ligands: Physiological importance and clinical implications. *Eur J Med Chem* 2019;166:502-13.
30. Christofides A, Konstantinidou E, Jani C, et al. The role of peroxisome proliferator-activated receptors (PPAR) in immune responses. *Metabolism* 2021;114:154338.
31. Lefere S, Puengel T, Hundertmark J, et al. Differential effects of selective- and pan-PPAR agonists on experimental steatohepatitis and hepatic macrophages☆. *J Hepatol* 2020;73:757-70.
32. Ni XX, Li XY, Wang Q, et al. Regulation of peroxisome proliferator-activated receptor-gamma activity affects the hepatic stellate cell activation and the progression of NASH via TGF- $\beta$ 1/Smad signaling pathway. *J Physiol Biochem* 2021;77:35-45.
33. Li X, Jin Q, Yao Q, et al. The Flavonoid Quercetin Ameliorates Liver Inflammation and Fibrosis by Regulating Hepatic Macrophages Activation and Polarization in Mice. *Front Pharmacol* 2018;9:72.
34. Wei Z, Zhao D, Zhang Y, et al. Rosiglitazone ameliorates bile duct ligation-induced liver fibrosis by down-regulating NF- $\kappa$ B-TNF- $\alpha$  signaling pathway in a PPAR $\gamma$ -dependent manner. *Biochem Biophys Res Commun* 2019;519:854-60.
35. Ye L, Chen T, Cao J, et al. Short hairpin RNA attenuates liver fibrosis by regulating the PPAR- $\gamma$  and NF- $\kappa$ B pathways in HBV-induced liver fibrosis in mice. *Int J Oncol* 2020;57:1116-28.

**Cite this article as:** Chen Q, Bao L, Lv L, Xie F, Zhou X, Zhang H, Zhang G. Schisandrin B regulates macrophage polarization and alleviates liver fibrosis via activation of PPAR $\gamma$ . *Ann Transl Med* 2021;9(19):1500. doi: 10.21037/atm-21-4602